



Transverse-spin-dependent azimuthal asymmetries of pion and kaon pairs produced in muon-proton and muon-deuteron semi-inclusive deep inelastic scattering

The COMPASS Collaboration

ARTICLE INFO

Article history:

Received 19 January 2023

Received in revised form 21 August 2023

Accepted 23 August 2023

Available online 29 August 2023

Editor: M. Doser

Keywords:

SIDIS

Di-hadron

Spin

Fragmentation

Transversity

Collins effect

ABSTRACT

A set of measurements of azimuthal asymmetries in the production of pairs of identified hadrons in deep-inelastic scattering of muons on transversely polarised ${}^6\text{LiD}$ (deuteron) and NH_3 (proton) targets is presented. All available data collected in the years 2003–2004 and 2007/2010 with the COMPASS spectrometer using a muon beam of 160 GeV/c at the CERN SPS were analysed. The asymmetries provide access to the transversity distribution functions via a fragmentation function that in principle may be independently obtained from e^+e^- annihilation data. Results are presented, discussed and compared to existing measurements as well as to model predictions. Asymmetries of $\pi^+\pi^-$ pairs measured with the proton target as a function of the Bjorken scaling variable are sizeable in the range $x > 0.032$, indicating non-vanishing transversity distribution and di-hadron interference fragmentation functions. As already pointed out by several authors, the small asymmetries of $\pi^+\pi^-$ measured on the ${}^6\text{LiD}$ target can be interpreted as indication for a cancellation of u and d -quark transversity distributions.

© 2023 The Author. Published by Elsevier B.V. This is an open access article under the CC BY license (<http://creativecommons.org/licenses/by/4.0/>). Funded by SCOAP³.

1. Introduction

The description of the nucleon spin structure remains one of the main challenges in hadron physics. For a polarised nucleon, a leading-twist description comprises eight transverse-momentum-dependent (TMD) parton distribution functions (PDFs), describing the distributions of longitudinal and transverse momenta of partons and their correlations with nucleon and quark polarisations [1]. After integration over quark intrinsic transverse momentum k_T , three PDFs fully describe the nucleon, *i.e.* the momentum distribution function $f_1^q(x)$, the helicity distribution function $g_1^q(x)$ and the transversity distribution function $h_1^q(x)$, where x denotes the Bjorken scaling variable. For simplicity, the latter will be referred to as “transversity” throughout this paper. While the momentum and the helicity distribution functions have been measured with good accuracy, the knowledge on transversity is inferior but steadily increasing. Unlike f_1^q and g_1^q , transversity is not accessible at leading twist in inclusive deep-inelastic scattering (DIS) because it is related to soft processes correlating quarks with opposite chirality, making it a chiral-odd function. Transversity can be accessed through observables that conserve chirality, *i.e.* when it is coupled to a chiral-odd partner. In this regard, measuring semi-inclusive deep-inelastic scattering (SIDIS) is advantageous as transversity is coupled to the chiral-odd fragmentation functions (FFs) that describe the hadronisation of a transversely polarised quark q into unpolarised final-state hadrons.

The major source of information on transversity has been measurements of transverse-spin-dependent asymmetries (TSAs) in single-hadron production in SIDIS ($\ell N^\uparrow \rightarrow \ell' h X$), where transversity is coupled to the Collins FF [2]. Transverse-spin asymmetries define the size of the transverse-target-spin-dependent azimuthal modulations of the SIDIS cross section. The first measurement of the Collins asymmetries was performed by the HERMES Collaboration [3] using a transversely polarised hydrogen target. Sizeable asymmetries were observed, suggesting non-zero transversity and Collins FFs. A major step forward came from measurements by the BELLE experiment [4,5] at the KEK e^+e^- collider, which detected azimuthal correlations of hadrons produced in opposite jets. This correlation involves the products or convolution of two Collins functions and was interpreted as a direct measure of the Collins effect. Later on the experiment performed measurements probing dihadron fragmentation functions [6,7], which play an important role in general understanding of hadronization processes and in the phenomenological extractions of the transversity PDFs. Further measurements have been provided by the BABAR [8,9] and the BE-SIII [10] experiments. The COMPASS Collaboration has the highest statistics data in this field, *e.g.* 28 M pion pairs taken with the NH_3 (proton) target and 4 M pion pairs taken with the ${}^6\text{LiD}$ (deuteron) target. The COMPASS collaboration has delivered a full set of measurements, *i.e.* both TSAs for unidentified charged hadrons [11] as well as pions and kaons [12] using the transversely polarised deuteron target, and TSAs for unidentified charged hadrons [13,14] as well as pions and kaons [15] using the transversely polarised

proton target. The TSAs measured with the polarised proton target showed a non-zero signal for Collins asymmetries with high statistics and a wide kinematic coverage. The TSAs measured with the polarised deuteron target are compatible with zero indicating a possible cancellation between up and down quark contributions to transversity. Despite the lower accuracy of these data, they were shown to play a key role in the extraction of flavour-dependent transversity distribution functions and remain the only SIDIS measurement ever performed using a transversely polarised deuteron target. In order to complete the COMPASS programme [16], a new high statistics measurement of TSAs using a transversely polarised deuteron target was performed in the last data taking campaign, in 2022.

A promising alternative approach to access transversity is the measurement of TSAs in semi-inclusive production of pairs of hadrons of opposite charge ($\ell^- N \rightarrow \ell^+ h^+ h^- X$). Following this approach, in this work $\pi^+ \pi^-$ and $K^+ K^-$ as well as $\pi^+ K^-$ and $K^+ \pi^-$ pairs will be studied. In this case, transversity is coupled to the chiral-odd interference fragmentation function (IFF) H_1^{\triangleleft} [17–19], which describes the hadronisation of a transversely polarised quark into a pair of unpolarised hadrons. At leading twist, and after integration over total transverse momentum, the differential cross section on a transversely polarised target comprises two terms and can be written as [20]

$$\frac{d^7\sigma}{d\cos\theta dM_{hh} d\phi_R dz dx dy d\phi_S} = \frac{\alpha^2}{2\pi Q^2 y} \left((1-y + \frac{y^2}{2}) \sum_q e_q^2 f_1^q(x) D_{1,q}(z, M_{hh}^2, \cos\theta) + S_{\perp}(1-y) \sum_q e_q^2 \frac{|\mathbf{p}_1 - \mathbf{p}_2|}{2M_{hh}} \sin\theta \sin\phi_{RS} h_1^q(x) H_{1,q}^{\triangleleft}(z, M_{hh}^2, \cos\theta) \right). \quad (1)$$

Here α is the fine-structure constant, $D_{1,q}(z, M_{hh}^2, \cos\theta)$ is the spin-independent dihadron fragmentation function (DiFF), y is the fraction of the lepton energy in the laboratory frame transferred to the exchanged virtual-photon and Q^2 the negative square of the four-momentum transfer. Here, z is the fraction of the virtual-photon energy carried by the hadron pair, M_{hh} its invariant mass and θ the polar angle of the positive hadron with respect to the two-hadron boost axis in the two-hadron rest frame. The symbol S_{\perp} denotes the component of the target spin vector \mathbf{S} perpendicular to the virtual-photon direction, with ϕ_S the azimuthal angle of the initial nucleon spin, $\phi_{S'}$ the azimuthal angle of the spin vector of the fragmenting quark and $\phi_{RS} = \phi_R - \phi_{S'} = \phi_R + \phi_S - \pi$. The azimuthal angle ϕ_R is given as

$$\phi_R = \frac{(\mathbf{q} \times \mathbf{l}) \cdot \mathbf{R}}{|\mathbf{q} \times \mathbf{l}| |\mathbf{q} \times \mathbf{R}|} \arccos \frac{(\mathbf{q} \times \mathbf{l}) \cdot (\mathbf{q} \times \mathbf{R})}{|\mathbf{q} \times \mathbf{l}| |\mathbf{q} \times \mathbf{R}|}, \quad (2)$$

where \mathbf{l} is the incoming lepton momentum, \mathbf{q} the virtual-photon momentum and \mathbf{R} the relative hadron momentum defined as $\mathbf{R} = (z_2 \mathbf{p}_1 - z_1 \mathbf{p}_2)/(z_1 + z_2)$, and 1 (2) denotes the positive (negative) hadron of the pair. The TSAs are experimentally accessible through the measured number of hadron pairs written as

$$N_{hh}(x, y, z, M_{hh}^2, \cos\theta, \phi_{RS}) \propto \sigma_{UU}(1 + f(x, y) P_T D_{nn}(y) A_{UT}^{\phi_{RS}} \sin\theta \sin\phi_{RS}), \quad (3)$$

where $f(x, y)$ is the target polarisation dilution factor, P_T the transverse polarisation of the target nucleons and D_{nn} the transverse-spin transfer coefficient. A more detailed discussion about the theoretical framework can be found in Ref. [21]. As shown in Ref. [21], the asymmetry

$$A_{UT}^{\sin\phi_{RS}} = \frac{|\mathbf{p}_1 - \mathbf{p}_2|}{2M_{hh}} \frac{\sum_q e_q^2 h_1^q(x) H_{1,q}^{\triangleleft}(z, M_{hh}^2, \cos\theta)}{\sum_q e_q^2 f_1^q(x) D_{1,q}(z, M_{hh}^2, \cos\theta)} \quad (4)$$

is proportional to the product of the transversity distribution function $h_1^q(x)$ and the polarised two-hadron interference fragmentation function $H_{1,q}^{\triangleleft}(z, M_{hh}^2, \cos\theta)$, summed over the quark flavours q with charge e_q .

Transverse-spin-dependent asymmetries of hadron pairs were first measured by the HERMES Collaboration [22] for pion pairs using a transversely polarised hydrogen target. A sizeable signal was seen as a function of x , indicating a sizeable u -quark transversity and non-vanishing interference fragmentation functions. The COMPASS collaboration has published measurements of transverse spin asymmetries for pairs of unidentified hadrons produced on polarised deuterons [21] and polarised protons [23]. The COMPASS results obtained with the proton target showed significantly sizeable asymmetries and a clear slope in their x -dependence thanks to the high accuracy of the proton data set, while those extracted from deuteron-target data were found to be compatible with zero. An intriguing similarity between Collins-like single-hadron asymmetries for the positive and negative hadrons extracted from the SIDIS hadron-pair data and the standard Collins asymmetries is observed as a function of x , suggesting that both single hadron and hadron-pair transverse-spin dependent fragmentation functions are generated by the same elementary mechanism, as presented and discussed in Ref. [24].

In this paper, we present a new measurement of TSAs for identified hadron-pairs using the full data set collected by the COMPASS Collaboration on transversely polarised deuteron (2003–2004) and proton (2007 and 2010) targets. The paper is organised as follows. Only a brief description of the experimental setup and data analysis are given in Sec. 3, as the same setup and methods of data cleaning, selection and extraction of TSAs as in previous COMPASS analyses [21,23] are used. The measured asymmetries are presented in Sec. 3 and discussed in Sec. 4.

2. Experimental data and analysis

The analysis presented in this paper is based on data collected in the years 2003–2004 and 2007/2010 using the COMPASS spectrometer [25] by scattering the naturally polarised μ^+ beam of 160 GeV/c delivered by the CERN SPS off transversely polarised ${}^6\text{LiD}$ and NH_3 targets, respectively. For ${}^6\text{LiD}$, the average dilution factor calculated for semi-inclusive reactions is $\langle f \rangle \sim 0.38$ and the average polarisation is $\langle P_T \rangle \sim 0.47$, while for NH_3 the corresponding values are $\langle f \rangle \sim 0.15$ and $\langle P_T \rangle \sim 0.83$, respectively. The target consisted of two or three cylindrical cells assembled in a row, which can be independently polarised. In 2003–2004, two cells were used, each 60 cm long and 3 cm in diameter, separated by a 10 cm gap. In 2007 and 2010, the target consisted of three cells of 4 cm diameter, with gaps of 5 cm in between. The middle cell was 60 cm long and the two outer ones 30 cm long each. From 2006 on, a new solenoidal magnet was used to polarise the target with a polar angle acceptance of 180 mrad as seen from the upstream end of the target, while in the earlier measurements with the ${}^6\text{LiD}$ target the polar angle acceptance was 70 mrad. For the measurement of transverse spin effects, the target material was polarised along the vertical direction. In order to reduce systematic effects, neighbouring cells were polarised in opposite directions allowing for simultaneous data taking with both target spin directions to reduce flux-dependent systematic uncertainties. Furthermore, the polarisation was destroyed and built up in reversed direction every four to five days, in order to cancel residual acceptance effects associated with the longitudinal position of the target cells (*i.e.* position along the beam line). For the data collected using a proton target, in the analysis, the central cell is divided into two parts,

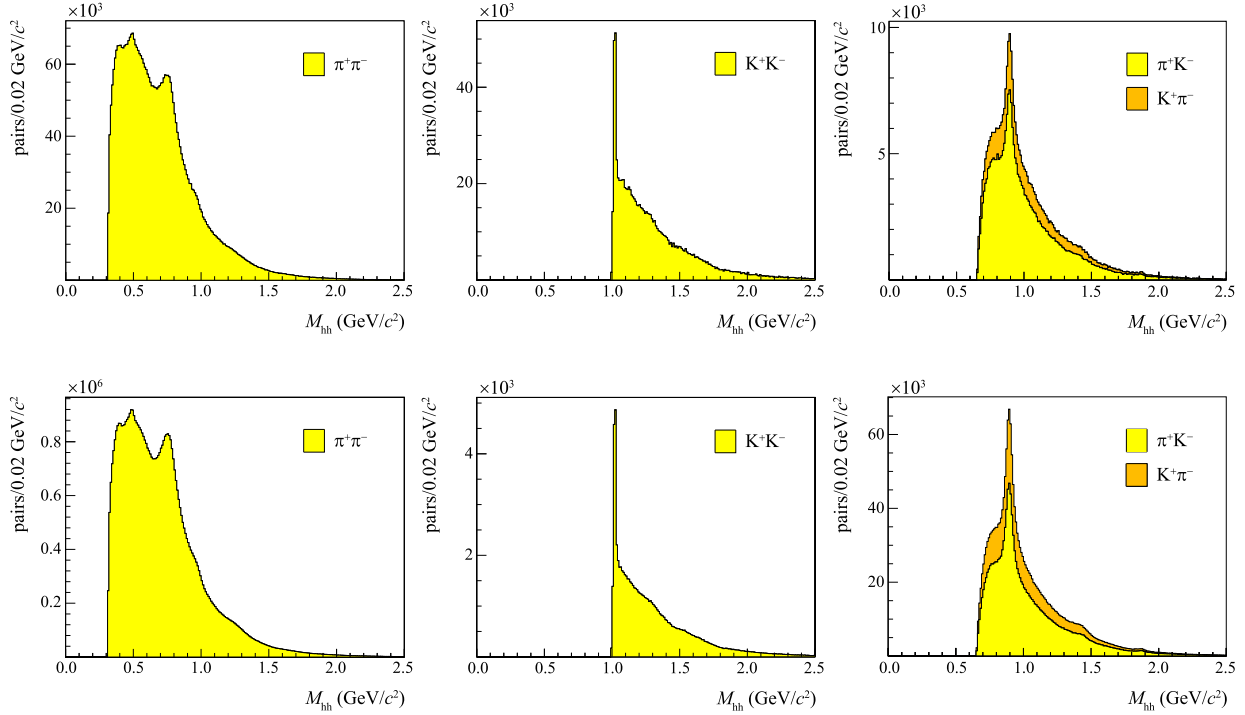


Fig. 1. Distributions of invariant mass M_{hh} for 2003-2004 deuteron data (top row) and combined 2007/2010 proton data (bottom row): $\pi^+\pi^-$ pairs (1st column), K^+K^- pairs (2nd column), π^+K^- and $K^+\pi^-$ pairs (3rd column).

providing four data samples with two different orientations of polarisation. Note that for the measurements in 2007 and in 2010 a similar spectrometer configuration was used.

In the analysis, events with incoming and outgoing muons and at least two reconstructed charged hadrons originating from the interaction vertex inside the target cells are selected. Equal flux through the whole target is obtained by requiring that the extrapolated beam tracks pass through all three cells. In order to select events in the DIS regime, requirements are applied on the squared four-momentum transfer, $Q^2 > 1$ $(\text{GeV}/c)^2$, and on the invariant mass of the final hadronic state, $W > 5$ GeV/c^2 . Furthermore, the fractional energy transfer to the virtual photon is required to be $y > 0.1$ and $y < 0.9$ to remove events with poorly reconstructed virtual-photon energy and events with large radiative corrections, respectively.

For a selected DIS event, all reconstructed hadrons originating from the interaction vertex are considered. Only hadrons produced in the current fragmentation region are selected by requiring $z > 0.1$ for the fractional energy and $x_F > 0.1$ for the Feynmann- x variable. The two-hadron sample consists of all combinations of oppositely charged hadrons built from the same DIS event. Exclusive dihadron production is suppressed by requiring the missing energy for each hadron pair to be greater than 3 GeV. As the azimuthal angle ϕ_R is only defined for non-collinear vectors \mathbf{R} and \mathbf{q} , a minimum value is required on the component of \mathbf{R} perpendicular to \mathbf{q} , i.e. $R_{\perp} > 0.07$ GeV/c . After the application of all requirements, 0.56×10^7 h^+h^- combinations remain for the deuteron data and 3.5×10^7 h^+h^- pairs for the proton data.

The RICH detector information is used to identify charged hadrons as pions or kaons in the momentum range between the Cherenkov threshold (about 2.6 GeV/c and 9 GeV/c , respectively) and 50 GeV/c . The detector set-up after the upgrade of 2005 and the particle identification (PID) procedure are fully described in Ref. [26], while details on the likelihood PID method and the purity of identified samples are explained in Ref. [12] and Ref. [15] for deuteron and proton targets, respectively. In the kinematic domain of the COMPASS experiment, about 67% of the final-state charged

Table 1

Final statistics for unidentified and identified charged-hadron pairs in deuteron (2003-2004) and proton (2007 and 2010) data.

Year	Number of pairs ($\times 10^6$)				
	h^+h^-	$\pi^+\pi^-$	π^+K^-	$K^+\pi^-$	K^+K^-
2003-2004 (deuteron)	5.65	3.97	0.26	0.30	0.10
2007 (proton)	10.91	7.41	0.38	0.53	0.22
2010 (proton)	34.56	20.60	1.10	1.53	0.60

hadrons are identified as pions and about 10% as kaons. The remaining particles are either protons, electrons or not clearly identified. About 60% are pion pairs ($\pi^+\pi^-$), about 2% are kaon pairs (K^+K^-) and about 8% are mixed pairs (π^+K^- , $K^+\pi^-$). The missing fraction refers to cases where at least one of the two hadrons cannot be accurately identified. The resulting statistics for unidentified and identified hadron pairs after applying all requirements are shown in Table 1.

The invariant-mass distributions for the four opposite-charge combinations that can be formed using identified charged pions and kaons ($\pi^+\pi^-$, K^+K^- , π^+K^- , $K^+\pi^-$) are shown in Fig. 1 for deuteron and proton targets. In the $\pi^+\pi^-$ spectrum, the mass signatures of some meson decays, such as K^0 around 500 MeV/c^2 ,¹ ρ^0 around 770 MeV/c^2 , f_0 around 980 MeV/c^2 and f_2 around 1270 MeV/c^2 , respectively, are clearly visible in both deuteron and proton data as expected from Ref. [27]. Other decays with more than two hadrons in the final state (like the decays of ω , η and η') generate broader peaks and contribute less to the overall pion-pair invariant-mass spectra [27]. The K^+K^- invariant-mass distribution shows a very pronounced signal of the $\phi(1020)$ resonance close to its production threshold. The ϕ meson can also contribute to the pion pair spectra via the two-step decay $\phi(1020) \rightarrow \rho\pi \rightarrow \pi^+\pi^-\pi^0$. The invariant-mass distribution

¹ The width and the number of the reconstructed K^0 are biased because in this analysis the pions are requested to come from a common interaction vertex inside the target.

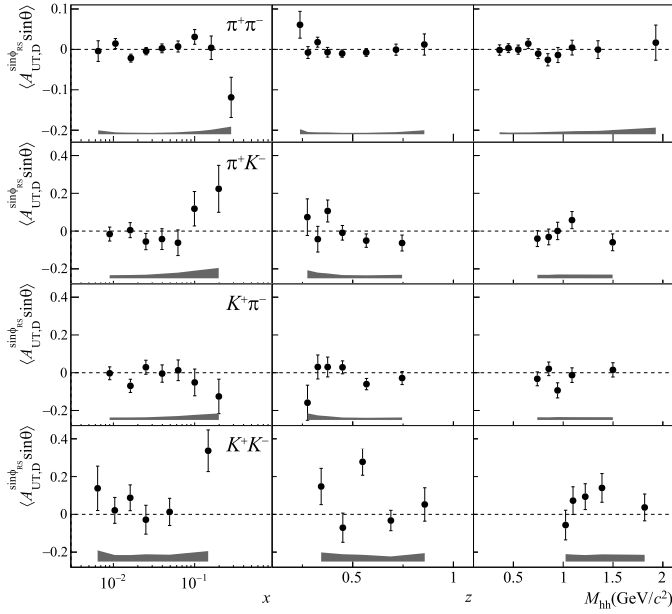


Fig. 2. Hadron-pair transverse-spin-dependent asymmetries as a function of x , z and M_{hh} , extracted from the full data set collected with the ${}^6\text{LiD}$ (deuteron) target. Systematic uncertainties are shown by the grey bands.

of K^+K^- pairs in the proton data shows indications of further broad peaks around $1300\text{ MeV}/c^2$ and $1500\text{ MeV}/c^2$, which might be caused by $f_2(1270)$ and $f_2'(1525)$. The invariant-mass distributions of π^+K^- and $K^+\pi^-$ also show in each case one dominant channel caused by the decays of $K^*(892)$. Further possible candidates for peaks in the M_{hh} spectra of the π^+K^- and $K^+\pi^-$ pairs are $K^*(1430)$ and $K_4^*(2045)$.

3. Results

The asymmetries were evaluated in bins of x , z and M_{hh} as given in Table 2. Several tests were performed to estimate the systematic uncertainties [23,15] which were evaluated to be at most 0.6 times the statistical ones. As in previous analysis [14,28,29], systematic effects due to a possible dependence of the efficiencies on the kinematic variables were estimated to be negligible and were not included. The asymmetries extracted from ${}^6\text{LiD}$ and NH_3 targets are presented in Figs. 2 and 3, respectively. The error bars indicate the statistical uncertainties while the grey bands show the systematic uncertainties. Numerical values of the asymmetries are available upon request.

For ${}^6\text{LiD}$, no significant asymmetry is observed in any variable for all pair combinations. For NH_3 , large negative asymmetries up to -0.07 are obtained for $\pi^+\pi^-$ pairs in the region $x > 0.03$, which implies that both transversity distributions and polarised two-hadron interference fragmentation functions do not vanish, as already observed in Refs. [22,23]. For $x < 0.03$, these asymmetries are compatible with zero.

The asymmetry measured with the ${}^6\text{LiD}$ target is compatible with zero within uncertainties over the whole x range. For both targets, no clear dependence on z can be observed, and for the NH_3 target the asymmetry is observed to be negative in the whole range. For both targets, the M_{hh} -dependence shows negative asymmetry values in the region of the ρ^0 mass.

For K^+K^- pairs, the proton data show negative asymmetries in all three variables, while the deuteron data show indications for a positive signal. In particular the M_{hh} -dependence shows opposite signs for the asymmetries measured with the NH_3 and ${}^6\text{LiD}$ target, with an indication of a mirror-symmetric shape. In the case of π^+K^- and $K^+\pi^-$ pairs, the deuteron data show asymmetries

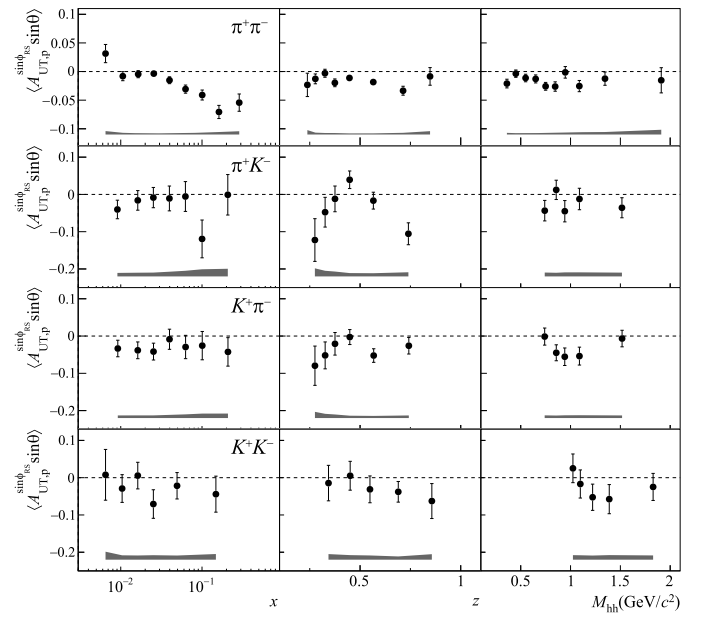


Fig. 3. Hadron-pair transverse-spin-dependent asymmetries as a function of x , z and M_{hh} , extracted from the full data set collected with the NH_3 (proton) target. Systematic uncertainties are shown by the grey bands.

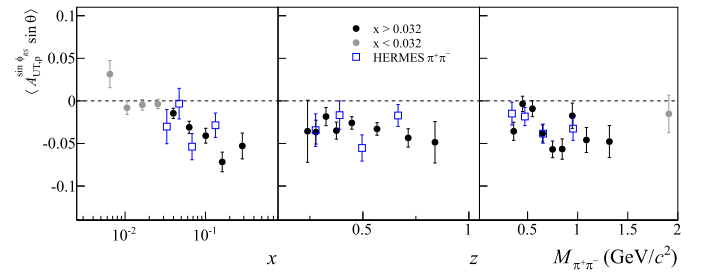


Fig. 4. Comparison of $\pi^+\pi^-$ pair asymmetries measured by the HERMES Collaboration [22] (blue open squares) with the results of the COMPASS Collaboration re-evaluated in the $x > 0.032$ region (black dots).

compatible with zero, while the proton data show slightly negative asymmetries.

The HERMES Collaboration measured TSAs for $\pi^+\pi^-$ pairs using electron-proton scattering [22]. Given the wider kinematic coverage by COMPASS, the $\pi^+\pi^-$ COMPASS asymmetry was re-evaluated in the region $x > 0.032$ to allow for a direct comparison. The comparison is shown in Fig. 4. The results are in very good agreement within statistical uncertainties.

4. Interpretation of the results

The dihadron fragmentation functions entering the SIDIS cross section in Eq. (1) are non-perturbative objects. As such, they can not be calculated from first principles. Two classes of models have been proposed to describe them. In spectator-jet type models a mechanism different from that of the Collins FF is invoked to produce a non-vanishing H_1^{\triangleleft} function. Such a mechanism involves the interference between the amplitudes of two competing channels for the production of the hadron pair, e.g. either the amplitude for direct production and the amplitude for resonance production [30,27], or the two amplitudes for the production of two different resonances [18]. A different approach is followed by the recursive string+ 3P_0 model of polarised quark fragmentation [31]. It is implemented in the StringSpinner package [32] for the simulation of the Collins effect for pseudoscalar mesons produced in

Table 2
Bin limits of the variables x , z and M_{hh} (in units of GeV/c^2) for the four types of pairs.

x bin limits										
$\pi\pi$	0.003	0.008	0.013	0.020	0.032	0.050	0.080	0.130	0.210	0.7
$\pi K/K\pi$	0.003	0.013	0.020	0.032	0.050	0.080	0.130	0.7		
KK	0.003	0.008	0.013	0.020	0.032	0.080	0.7			
z bin limits										
$\pi\pi$	0.20	0.25	0.30	0.35	0.40	0.50	0.65	0.80	1.0	
$\pi K/K\pi$	0.20	0.30	0.35	0.40	0.50	0.65	1.0			
KK	0.20	0.40	0.50	0.65	0.80	1.0				
M _{hh} bin limits										
$\pi\pi$	0.0	0.4	0.5	0.6	0.7	0.8	0.9	1.0	1.2	1.6
$\pi K/K\pi$	0.0	0.8	0.9	1.0	1.2	10				
KK	0.9	1.05	1.15	1.30	1.50	10				

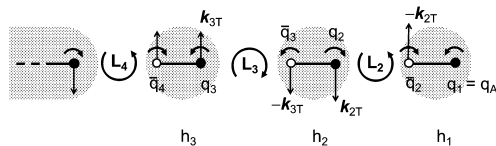


Fig. 5. The string+ 3P_0 mechanism of polarised quark fragmentation [34]. The closed (open) circles represent quark (antiquarks) at the string ends. The circular arrows above quarks show the orientation of their spins whereas the arrows at each string breaking $L_2, L_3 \dots$ represent the orientation of the relative orbital angular momentum of the $q\bar{q}$ pairs. The straight arrows indicate the quark transverse momenta.

the fragmentation of transversely polarised quarks in SIDIS with the PYTHIA 8 event generator [33].

The classical string+ 3P_0 model for the fragmentation of a transversely polarised quark q_A is illustrated in Fig. 5. The string is stretched between the scattered quark q_A and the target remnants along the quark direction and the string fragmentation occurs via tunnelling of quark-antiquark pairs in the 3P_0 state, *i.e.* with spin $S = 1$ and relative orbital angular momentum $L = 1$, such that the total angular momentum J is zero. Given the polarisation of q_A , taken here along the normal to the figure plane, at the string breakings the spin and the transverse momentum of the quark and antiquark, as well as the transverse momentum of the produced hadron are fixed. The rank r indicates how far the hadron h_r is produced from the fragmenting quark q_A , with h_1 being the hadron which contains q_A . For odd (even) r the hadron h_r is emitted to the left (right) with respect to the plane spanned by the momentum and polarisation vectors of the fragmenting quark. As an example, if the flavor of the fragmenting quark is $q_A = u$ and $h_1 = \pi^+$, it can be $h_2 = \pi^-$ and opposite Collins asymmetries for oppositely charged hadrons are generated. Also, a dihadron asymmetry with the same sign as for positive hadrons is produced. StringSpinner uses the quantum mechanical formulation of this model, in which the spin effects depend on a complex parameter, tuned as in Ref. [32]. The initial quark polarisation is given by a parametrisation of the transversity PDF for valence u and d quarks. For this work we have used the default parametrisations, which were tuned to reproduce the π^+ and π^- Collins asymmetries measured by COMPASS on an NH_3 target. The simulations were performed neglecting the intrinsic transverse momentum of the quarks, but it was checked that the dihadron asymmetries are not affected [34].

In Fig. 6 the measured dihadron asymmetries (closed points) are compared to the simulated asymmetries (open points) for proton data. As can be seen, the simulation describes the data particularly well for $\pi^+\pi^-$ and K^+K^- pairs, in all kinematic variables. The trend of the asymmetries as a function of x is mainly driven by the x -shape of the implemented transversity PDFs, while the z and M_{hh} dependences are predictions of the model. The large signal

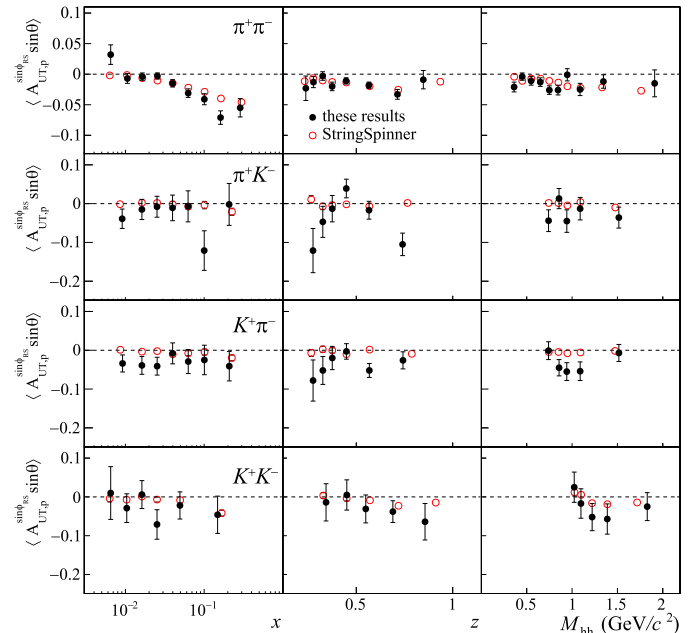


Fig. 6. Comparison between $\pi^+\pi^-$, π^+K^- , $K^+\pi^-$ and K^+K^- asymmetries for proton data (closed points) and results from simulations using StringSpinner (open points).

for $\pi^+\pi^-$ and K^+K^- pairs can be understood in the approximation of u -quark dominance considering the fact that π^+ or K^+ are most likely produced at rank one, whereas π^- or K^- are produced at rank two. Regarding the π^+K^- and $K^+\pi^-$ pairs, the simulated asymmetries are small and compatible with the data within uncertainties. This is expected considering the fact that, *e.g.*, the π^+ and the K^- of a π^+K^- pair are most likely produced at rank one and three separated by a rank two neutral kaon. Thus the π^+ and the K^- are most likely emitted on the same side producing a small dihadron asymmetry.

In corresponding simulations for deuteron data, dihadron asymmetries compatible with zero were found for all types of hadron pairs. This is in agreement with the data and is expected from the fact that the transversity PDFs for valence u and d -quarks have almost the same size but opposite sign.

5. Conclusions

In this paper we present the results of a new measurement of transverse-spin-dependent asymmetries in hadron pair production in DIS of 160 GeV/c muons off transversely polarised deuteron (${}^6\text{LiD}$) and proton (NH_3) targets. The measurement covers all pos-

sible combinations of oppositely charged pions and kaons observed in the COMPASS kinematic range.

The deuteron data used in the analysis were collected during 2003 and 2004, while the proton data include two separate parts collected in 2007 and 2010. Both data sets were already used earlier to extract the Collins and Sivers asymmetries for semi-inclusively measured single hadrons, with separate publications for charged hadrons as well for identified pions and kaons. These two data sets are the largest ones available on this process, including e.g. 28M (4M) pion pairs in the proton (deuteron) data, and they provide important input for global analyses.

The proton data show significant non-zero asymmetries. For $\pi^+\pi^-$ pairs, values reach -7% in the region $x > 0.032$ and -2.5% in the invariant-mass region around the ρ^0 -meson mass. Slightly negative asymmetries are observed for K^+K^- and $K^+\pi^-$ pairs. The deuteron data show for all hadron combinations asymmetries compatible with zero, within statistical uncertainties.

Declaration of competing interest

The authors declare that they have no known competing financial interests or personal relationships that could have appeared to influence the work reported in this paper.

Data availability

The authors are unable or have chosen not to specify which data has been used.

Acknowledgements

This work was made possible thanks to the financial support of our funding agencies. We also acknowledge the support of the CERN management and staff, as well as the skills and efforts of the technicians of the collaborating institutes.

References

- [1] M. Anselmino, A. Mukherjee, A. Vossen, Transverse spin effects in hard semi-inclusive collisions, *Prog. Part. Nucl. Phys.* 114 (2020) 103806, <https://doi.org/10.1016/j.ppnp.2020.103806>, arXiv:2001.05415.
- [2] J.C. Collins, Fragmentation of transversely polarized quarks probed in transverse momentum distributions, *Nucl. Phys. B* 396 (1993) 161–182, [https://doi.org/10.1016/0550-3213\(93\)90262-N](https://doi.org/10.1016/0550-3213(93)90262-N), arXiv:hep-ph/9208213.
- [3] A. Airapetian, et al., Single-spin asymmetries in semi-inclusive deep-inelastic scattering on a transversely polarized hydrogen target, *Phys. Rev. Lett.* 94 (2005) 012002, <https://doi.org/10.1103/PhysRevLett.94.012002>, arXiv:hep-ex/0408013.
- [4] K. Abe, et al., Measurement of azimuthal asymmetries in inclusive production of hadron pairs in e^+e^- annihilation at Belle, *Phys. Rev. Lett.* 96 (2006) 232002, <https://doi.org/10.1103/PhysRevLett.96.232002>, arXiv:hep-ex/0507063.
- [5] R. Seidl, et al., Measurement of azimuthal asymmetries in inclusive production of hadron pairs in e^+e^- annihilation at $s^{**}(1/2) = 10.58$ -GeV, *Phys. Rev. D* 78 (2008) 032011, <https://doi.org/10.1103/PhysRevD.78.032011>, Erratum: *Phys. Rev. D* 86 (2012) 039905, arXiv:0805.2975.
- [6] A. Vossen, et al., Observation of transverse polarization asymmetries of charged pion pairs in e^+e^- annihilation near $\sqrt{s} = 10.58$ GeV, *Phys. Rev. Lett.* 107 (2011) 072004, <https://doi.org/10.1103/PhysRevLett.107.072004>, arXiv:1104.2425.
- [7] R. Seidl, et al., Invariant-mass and fractional-energy dependence of inclusive production of di-hadrons in e^+e^- annihilation at $\sqrt{s} = 10.58$ GeV, *Phys. Rev. D* 96 (3) (2017) 032005, <https://doi.org/10.1103/PhysRevD.96.032005>, arXiv:1706.08348.
- [8] J.P. Lees, et al., Measurement of Collins asymmetries in inclusive production of charged pion pairs in e^+e^- annihilation at BABAR, *Phys. Rev. D* 90 (5) (2014) 052003, <https://doi.org/10.1103/PhysRevD.90.052003>, arXiv:1309.5278.
- [9] J.P. Lees, et al., Collins asymmetries in inclusive charged KK and $K\pi$ pairs produced in e^+e^- annihilation, *Phys. Rev. D* 92 (11) (2015) 111101, <https://doi.org/10.1103/PhysRevD.92.111101>, arXiv:1506.05864.
- [10] M. Ablikim, et al., Measurement of azimuthal asymmetries in inclusive charged dipion production in e^+e^- annihilations at $\sqrt{s} = 3.65$ GeV, *Phys. Rev. Lett.* 116 (4) (2016) 042001, <https://doi.org/10.1103/PhysRevLett.116.042001>, arXiv:1507.06824.
- [11] V. Alexakhin, et al., First measurement of the transverse spin asymmetries of the deuteron in semi-inclusive deep inelastic scattering, *Phys. Rev. Lett.* 94 (2005) 202002, <https://doi.org/10.1103/PhysRevLett.94.202002>, arXiv:hep-ex/0503002.
- [12] M. Alekseev, et al., Collins and Sivers asymmetries for pions and kaons in muon-deuteron DIS, *Phys. Lett. B* 673 (2009) 127–135, <https://doi.org/10.1016/j.physletb.2009.01.060>, arXiv:0802.2160.
- [13] M. Alekseev, et al., Measurement of the Collins and Sivers asymmetries on transversely polarised protons, *Phys. Lett. B* 692 (2010) 240–246, <https://doi.org/10.1016/j.physletb.2010.08.001>, arXiv:1005.5609.
- [14] C. Adolph, et al., Experimental investigation of transverse spin asymmetries in muon-p SIDIS processes: Collins asymmetries, *Phys. Lett. B* 717 (2012) 376–382, <https://doi.org/10.1016/j.physletb.2012.09.055>, arXiv:1205.5121.
- [15] C. Adolph, et al., Collins and Sivers asymmetries in muon production of pions and kaons off transversely polarised protons, *Phys. Lett. B* 744 (2015) 250–259, <https://doi.org/10.1016/j.physletb.2015.03.056>, arXiv:1408.4405.
- [16] K. Augsten, et al. (COMPASS Collaboration), *Addendum to COMPASS II proposal, d-Quark Transversity and Proton Radius, CERN-SPSC-2017-034 SPSC-P-340-ADD-1* (2018).
- [17] J.C. Collins, S.F. Heppelmann, G.A. Ladinsky, Measuring transversity densities in singly polarized hadron - hadron and lepton - hadron collisions, *Nucl. Phys. B* 420 (1994) 565–582, [https://doi.org/10.1016/0550-3213\(94\)90078-7](https://doi.org/10.1016/0550-3213(94)90078-7), arXiv:hep-ph/9305309.
- [18] R.L. Jaffe, X.-m. Jin, J. Tang, Interference fragmentation functions and the nucleon's transversity, *Phys. Rev. Lett.* 80 (1998) 1166–1169, <https://doi.org/10.1103/PhysRevLett.80.1166>, arXiv:hep-ph/9709322.
- [19] A. Bianconi, S. Boffi, R. Jakob, M. Radici, Two hadron interference fragmentation functions. Part 1. General framework, *Phys. Rev. D* 62 (2000) 034008, <https://doi.org/10.1103/PhysRevD.62.034008>, arXiv:hep-ph/9907475.
- [20] A. Bacchetta, M. Radici, Partial wave analysis of two hadron fragmentation functions, *Phys. Rev. D* 67 (2003) 094002, <https://doi.org/10.1103/PhysRevD.67.094002>, arXiv:hep-ph/0212300.
- [21] C. Adolph, et al., Transverse spin effects in hadron-pair production from semi-inclusive deep inelastic scattering, *Phys. Lett. B* 713 (2012) 10–16, <https://doi.org/10.1016/j.physletb.2012.05.015>, arXiv:1202.6150.
- [22] A. Airapetian, et al., Evidence for a transverse single-spin asymmetry in lepton production of $\pi^+\pi^-$ pairs, *J. High Energy Phys.* 06 (2008) 017, <https://doi.org/10.1088/1126-6708/2008/06/017>, arXiv:0803.2367.
- [23] C. Adolph, et al., A high-statistics measurement of transverse spin effects in dihadron production from muon-proton semi-inclusive deep-inelastic scattering, *Phys. Lett. B* 736 (2014) 124–131, <https://doi.org/10.1016/j.physletb.2014.06.080>, arXiv:1401.7873.
- [24] C. Adolph, et al., Interplay among transversity induced asymmetries in hadron lepton production, *Phys. Lett. B* 753 (2016) 406–411, <https://doi.org/10.1016/j.physletb.2015.12.042>, arXiv:1507.07593.
- [25] P. Abbon, et al., The COMPASS experiment at CERN, *Nucl. Instrum. Methods, Sect. A* 577 (2007) 455–518, <https://doi.org/10.1016/j.nima.2007.03.026>, arXiv:hep-ex/0703049.
- [26] P. Abbon, et al., Particle identification with compass rich-1, *Nucl. Instrum. Methods, Sect. A* 631 (1) (2011) 26–39, <https://doi.org/10.1016/j.nima.2010.11.106>, <http://www.sciencedirect.com/science/article/pii/S0168900210026422>.
- [27] A. Bacchetta, M. Radici, Modeling dihadron fragmentation functions, *Phys. Rev. D* 74 (2006) 114007, <https://doi.org/10.1103/PhysRevD.74.114007>, arXiv:hep-ph/0608037.
- [28] C. Adolph, et al., II – Experimental investigation of transverse spin asymmetries in μ -p SIDIS processes: Sivers asymmetries, *Phys. Lett. B* 717 (2012) 383–389, <https://doi.org/10.1016/j.physletb.2012.09.056>, arXiv:1205.5122.
- [29] M.G. Alexeev, et al., Measurement of P_T -weighted Sivers asymmetries in lepton production of hadrons, *Nucl. Phys. B* 940 (2019) 34–53, <https://doi.org/10.1016/j.nuclphysb.2018.12.024>, arXiv:1809.02936.
- [30] J.C. Collins, G.A. Ladinsky, On π - π correlations in polarized quark fragmentation using the linear sigma model, [arXiv:hep-ph/9411444](https://arxiv.org/abs/hep-ph/9411444), Dec. 1994.
- [31] A. Kerbizi, X. Artru, Z. Belghobsi, A. Martin, Simplified recursive 3P_0 model for the fragmentation of polarized quarks, *Phys. Rev. D* 100 (1) (2019) 014003, <https://doi.org/10.1103/PhysRevD.100.014003>, arXiv:1903.01736.
- [32] A. Kerbizi, L. Lönnblad, StringSpinner - adding spin to the PYTHIA string fragmentation, *Comput. Phys. Commun.* 272 (2022) 108234, <https://doi.org/10.1016/j.cpc.2021.108234>, arXiv:2105.09730.
- [33] T. Sjostrand, S. Mrenna, P.Z. Skands, A brief introduction to PYTHIA 8.1, *J. High Energy Phys.* 05 (2006) 026, *Comput. Phys. Commun.* 178 (2008) 852–867, <https://doi.org/10.1016/j.cpc.2008.01.036>, arXiv:0710.3820.
- [34] A. Kerbizi, X. Artru, Z. Belghobsi, F. Bradamante, A. Martin, Recursive model for the fragmentation of polarized quarks, *Phys. Rev. D* 97 (7) (2018) 074010, <https://doi.org/10.1103/PhysRevD.97.074010>, arXiv:1802.00962.

The COMPASS Collaboration

G.D. Alexeev ^{30, ID}, M.G. Alexeev ^{21,20, ID}, C. Alice ^{21,20, ID}, A. Amoroso ^{21,20, ID}, V. Andrieux ^{34, ID}, V. Anosov ^{30, ID}, K. Augsten ^{4, ID}, W. Augustyniak ²⁵, C.D.R. Azevedo ^{28, ID}, B. Badelek ^{27, ID}, J. Barth ^{8, ID}, R. Beck ⁸, Y. Bedfer ^{6, ID}, J. Bernhard ^{12,32, ID}, M. Bodlak ⁵, F. Bradamante ^{18, ID}, C. Braun ¹⁰, A. Bressan ^{19,18, ID}, V.E. Burtsev ³¹, W.-C. Chang ^{33, ID}, C. Chatterjee ^{18, ID, a}, M. Chiosso ^{21,20, ID}, A.G. Chumakov ^{31, ID}, S.-U. Chung ^{13,k,k1}, A. Cicuttin ^{18,17, ID}, P.M.M. Correia ^{28, ID}, M.L. Crespo ^{18,17, ID}, D' Ago ^{19,18, ID}, S. Dalla Torre ^{18, ID}, S.S. Dasgupta ¹⁵, S. Dasgupta ^{18, ID, g}, F. Del Carro ^{21,20, ID}, I. Denisenko ^{30, ID}, O.Yu. Denisov ^{20, ID}, S.V. Donskov ^{31, ID}, N. Doshita ^{24, ID}, Ch. Dreisbach ^{13, ID}, W. Dünnweber ^{ID, d, d1}, R.R. Dusaev ^{31, ID}, D. Ecker ^{13, ID}, A. Efremov ^{30, †}, C. Elia ^{19,18, ID}, D. Eremeev ³¹, P. Faccioli ^{29, ID}, M. Faessler ^{d, d1}, M. Finger ^{5, ID}, M. Finger jr. ^{5, ID}, H. Fischer ^{11, ID}, K.J. Flöthner ^{8, ID}, W. Florian ^{18,17, ID}, J.M. Friedrich ^{13, ID}, V. Frolov ^{30,32, ID}, L.G. Garcia Ordóñez ^{18,17, ID}, F. Gautheron ^{7,34, ID}, O.P. Gavrichtchouk ^{30, ID}, S. Gerassimov ^{31,13, ID}, J. Giarra ^{12, ID}, D. Giordano ^{21,20, ID}, M. Gorzellik ^{11, ID, c}, A. Grasso ^{21,20}, A. Gridin ^{30, ID}, M. Grosse Perdekamp ^{34, ID}, B. Grube ^{13, ID}, M. Grüner ^{8, ID}, A. Guskov ^{30, ID}, D. von Harrach ¹², M. Hoffmann ^{8, ID, a}, N. Horikawa ^{23, i}, N. d'Hose ^{6, ID}, C.-Y. Hsieh ^{33, ID, l}, S. Huber ¹³, S. Ishimoto ^{24, ID, j}, A. Ivanov ³⁰, T. Iwata ^{24, ID}, M. Jandek ⁴, V. Jary ^{4, ID}, R. Joosten ^{8, ID}, E. Kabuß ^{12, ID}, F. Kaspar ^{13, ID}, A. Kerbizi ^{19,18, ID}, B. Ketzer ^{8, ID}, A. Khatun ^{6, ID}, G.V. Khaustov ^{31, ID}, F. Klein ⁹, J.H. Koivuniemi ^{7,34, ID}, V.N. Kolosov ^{31, ID}, K. Kondo Horikawa ^{24, ID}, I. Konorov ^{31,13, ID}, V.F. Konstantinov ^{31, †}, A.M. Korzenev ^{30, ID}, A.M. Kotzinian ^{1,20, ID}, O.M. Kouznetsov ^{30, ID}, A. Koval ²⁵, Z. Kral ^{5, ID}, F. Krinner ¹³, F. Kunne ⁶, K. Kurek ^{25, ID}, R.P. Kurjata ^{26, ID}, A. Kveton ^{5, ID}, K. Lavickova ^{4, ID}, S. Levorato ^{32,18, ID}, Y.-S. Lian ^{33, ID, m}, J. Lichtenstadt ^{16, ID}, P.-J. Lin ^{33, ID, b}, R. Longo ^{34, ID}, V.E. Lyubovitskij ^{31, ID, f}, A. Maggiora ^{20, ID}, A. Magnon ^{15, †}, N. Makins ³⁴, N. Makke ^{18, ID, *,}, G.K. Mallot ^{32,11, ID}, A. Maltsev ^{30, ID}, S.A. Mamon ³¹, A. Martin ^{19,18, ID}, J. Marzec ^{26, ID}, J. Matoušek ^{5, ID}, T. Matsuda ^{22, ID}, G. Mattson ^{34, ID}, C. Menezes Pires ^{29, ID}, F. Metzger ^{8, ID}, M. Meyer ^{34,6, ID}, W. Meyer ⁷, Yu.V. Mikhailov ^{31, †}, M. Mikhasenko ^{14, ID, e}, E. Mitrofanov ³⁰, D. Miura ^{24, ID}, Y. Miyachi ^{24, ID}, R. Molina ^{18,17, ID}, A. Moretti ^{19,18, ID}, A. Nagaytsev ^{30, ID}, D. Neyret ^{6, ID}, M. Niemiec ^{27, ID}, J. Nový ^{4, ID}, W.-D. Nowak ^{12, ID}, G. Nukazuka ^{24, ID}, A.G. Olshevsky ^{30, ID}, M. Ostrick ^{12, ID}, D. Panzieri ^{20, ID, h, h1}, B. Parsamyan ^{1,20, ID, *,}, S. Paul ^{13, ID}, H. Pekeler ^{8, ID}, J.-C. Peng ^{34, ID}, G. Pesaro ^{19,18}, M. Pešek ^{5, ID}, D.V. Peshekhonov ^{30, ID}, M. Pešková ^{5, ID}, S. Platchkov ^{6, ID}, J. Pochodzalla ^{12, ID}, V.A. Polyakov ^{31, ID}, M. Quaresma ^{29, ID}, C. Quintans ^{29, ID}, G. Reicherz ^{7, ID}, C. Riedl ^{34, ID}, D.I. Ryabchikov ^{31,13, ID}, A. Rychter ^{26, ID}, A. Rymbekova ³⁰, V.D. Samoylenko ^{31, ID}, A. Sandacz ^{25, ID}, S. Sarkar ^{15, ID}, I.A. Savin ^{30, ID, †}, G. Sbrizzai ^{18, ID}, P. Schiavon ^{19,18}, H. Schmieden ⁹, A. Selyunin ^{30, ID}, K. Sharko ^{31, ID}, L. Sinha ¹⁵, M. Slunecka ^{30,5, ID}, F. Sozzi ^{18, ID}, D. Spülbeck ^{8, ID}, A. Srnka ^{2, ID}, M. Stolarski ^{29, ID}, O. Subrt ^{32,4, ID}, M. Sulc ^{3, ID}, H. Suzuki ^{24, ID, i}, S. Tessaro ^{18, ID}, F. Tessarotto ^{18, ID, *,}, A. Thiel ^{8, ID}, J. Tomsa ^{5, ID}, F. Tosello ^{20, ID}, A. Townsend ^{34, ID}, T. Triloki ^{18, ID, a}, V. Tskhay ^{31, ID}, B. Valinoti ^{18,17, ID}, B.M. Veit ^{12, ID}, J.F.C.A. Veloso ^{28, ID}, B. Ventura ⁶, M. Virius ^{4, ID}, M. Wagner ^{8, ID}, S. Wallner ^{13, ID}, K. Zaremba ^{26, ID}, M. Zavertyaev ^{31, ID}, M. Zemko ^{5,4, ID}, E. Zemlyanichkina ^{30, ID}, M. Ziembicki ^{26, ID}

¹ A.I. Alikhanyan National Science Laboratory, 2 Alikhanyan Br. Street, 0036, Yerevan, Armenia² Institute of Scientific Instruments of the CAS, 61264 Brno, Czech Republic ^A³ Technical University in Liberec, 46117 Liberec, Czech Republic ^A⁴ Czech Technical University in Prague, 16636 Prague, Czech Republic ^A⁵ Charles University, Faculty of Mathematics and Physics, 12116 Prague, Czech Republic ^A⁶ IRFU, CEA, Université Paris-Saclay, 91191 Gif-sur-Yvette, France⁷ Universität Bochum, Institut für Experimentalphysik, 44780 Bochum, Germany ^B⁸ Universität Bonn, Helmholtz-Institut für Strahlen- und Kernphysik, 53115 Bonn, Germany ^B⁹ Universität Bonn, Physikalisches Institut, 53115 Bonn, Germany ^B¹⁰ Universität Erlangen-Nürnberg, Physikalisches Institut, 91054 Erlangen, Germany

¹¹ Universität Freiburg, Physikalisches Institut, 79104 Freiburg, Germany ^B
¹² Universität Mainz, Institut für Kernphysik, 55099 Mainz, Germany ^B
¹³ Technische Universität München, Physik Dept., 85748 Garching, Germany ^B
¹⁴ Ludwig-Maximilians-Universität, 80539 München, Germany
¹⁵ Matrivani Institute of Experimental Research & Education, Calcutta-700 030, India ^C
¹⁶ Tel Aviv University, School of Physics and Astronomy, 69978 Tel Aviv, Israel ^D
¹⁷ Abdus Salam ICTP, 34151 Trieste, Italy
¹⁸ Trieste Section of INFN, 34127 Trieste, Italy
¹⁹ University of Trieste, Dept. of Physics, 34127 Trieste, Italy
²⁰ Torino Section of INFN, 10125 Torino, Italy
²¹ University of Torino, Dept. of Physics, 10125 Torino, Italy
²² University of Miyazaki, Miyazaki 889-2192, Japan ^E
²³ Nagoya University, 464 Nagoya, Japan ^E
²⁴ Yamagata University, Yamagata 992-8510, Japan ^E
²⁵ National Centre for Nuclear Research, 02-093 Warsaw, Poland ^F
²⁶ Warsaw University of Technology, Institute of Radioelectronics, 00-665 Warsaw, Poland ^F
²⁷ University of Warsaw, Faculty of Physics, 02-093 Warsaw, Poland ^F
²⁸ University of Aveiro, 3810-193 Aveiro, Portugal ^G
²⁹ LIP, 1649-003 Lisbon, Portugal ^G
³⁰ Affiliated with an international laboratory covered by a cooperation agreement with CERN
³¹ Affiliated with an institute covered by a cooperation agreement with CERN
³² CERN, 1211 Geneva 23, Switzerland
³³ Academia Sinica, Institute of Physics, Taipei 11529, Taiwan ^H
³⁴ University of Illinois at Urbana-Champaign, Dept. of Physics, Urbana, IL 61801-3080, USA ^I

* Corresponding authors N. Makke, B. Parsamyan, F. Tessarotto.

E-mail addresses: nour.makke@cern.ch (N. Makke), bakur.parsamyan@cern.ch (B. Parsamyan), fulvio.tessarotto@ts.infn.it (F. Tessarotto).

^a Supported by the European Union's Horizon 2020 research and innovation programme under grant agreement STRONG-2020 - No 824093.

^b Supported by ANR, France with P2IO LabEx (ANR-10-LABX-0038) in the framework "Investissements d'Avenir" (ANR-11-IDEX-0003-01).

^c Supported by the DFG Research Training Group Programmes 1102 and 2044 (Germany).

^d Retired from Ludwig-Maximilians-Universität, 80539 München, Germany.

^{d1} Supported by the DFG cluster of excellence 'Origin and Structure of the Universe' (www.universe-cluster.de) (Germany).

^e Also at ORIGINS Excellence Cluster, 85748 Garching, Germany.

^f Also at Institut für Theoretische Physik, Universität Tübingen, 72076 Tübingen, Germany.

^g Present address: NISER, Centre for Medical and Radiation Physics, Bhubaneswar, India.

^h Also at University of Eastern Piedmont, 15100 Alessandria, Italy.

^{h1} Supported by the Funds for Research 2019-22 of the University of Eastern Piedmont.

ⁱ Also at Chubu University, Kasugai, Aichi 487-8501, Japan.

^j Also at KEK, 1-1 Oho, Tsukuba, Ibaraki 305-0801, Japan.

^k Also at Dept. of Physics, Pusan National University, Busan 609-735, Republic of Korea.

^{k1} Also at Physics Dept., Brookhaven National Laboratory, Upton, NY 11973, USA.

^l Also at Dept. of Physics, National Central University, 300 Jhongda Road, Jhongli 32001, Taiwan.

^m Also at Dept. of Physics, National Kaohsiung Normal University, Kaohsiung County 824, Taiwan.

[†] Deceased.

^A Supported by MEYS, Grants LM2015058, LM2018104 and LTT17018 and Charles University Grant PRIMUS/22/SCI/017 (Czech Republic).

^B Supported by BMBF - Bundesministerium für Bildung und Forschung (Germany).

^C Supported by B. Sen fund (India).

^D Supported by the Israel Academy of Sciences and Humanities (Israel).

^E Supported by MEXT and JSPS, Grants 18002006, 20540299, 18540281 and 26247032, the Daiko and Yamada Foundations (Japan).

^F Supported by NCN, Grant 2020/37/B/ST2/01547 (Poland).

^G Supported by FCT, Grants CERN/FIS-PAR/0022/2019 and CERN/FIS-PAR/0016/2021 (Portugal).

^H Supported by the Ministry of Science and Technology (Taiwan).

^I Supported by the National Science Foundation, Grant no. PHY-1506416 (USA).